

Published in final edited form as:

Mol Ther. 2009 December ; 17(12): 2041–2048. doi:10.1038/mt.2009.218.

## Noninvasive Imaging and Radiovirotherapy of Prostate Cancer Using an Oncolytic Measles Virus Expressing the Sodium Iodide Symporter

Pavlos Msaouel<sup>1,2</sup>, Ianko D Iankov<sup>1</sup>, Cory Allen<sup>1</sup>, Ileana Aderca<sup>1</sup>, Mark J Federspiel<sup>1</sup>, Donald J Tindall<sup>3</sup>, John C Morris<sup>4</sup>, Michael Koutsilieris<sup>2</sup>, Stephen J Russell<sup>1</sup>, and Evanthia Galanis<sup>1,5</sup>

<sup>1</sup> Department of Molecular Medicine, Mayo Clinic, Rochester, Minnesota, USA

<sup>2</sup> Department of Experimental Physiology, National and Kapodistrian University of Athens, Athens, Greece

<sup>3</sup> Department of Urology Research, Mayo Clinic, Rochester, Minnesota, USA

<sup>4</sup> Department of Internal Medicine, Division of Endocrinology, Diabetes, Metabolism, Nutrition, Mayo Clinic, Rochester, Minnesota, USA

<sup>5</sup> Division of Medical Oncology, Mayo Clinic, Rochester, Minnesota, USA

### Abstract

Prostate cancer cells overexpress the measles virus (MV) receptor CD46. Herein, we evaluated the antitumor activity of an oncolytic derivative of the MV Edmonston (MV-Edm) vaccine strain engineered to express the human sodium iodide symporter (NIS; MV-NIS virus). MV-NIS showed significant cytopathic effect (CPE) against prostate cancer cell lines *in vitro*. Infected cells effectively concentrated radioiodide isotopes as measured *in vitro* by Iodide-125 (<sup>125</sup>I) uptake assays. Virus localization and spread *in vivo* could be effectively followed by imaging of <sup>123</sup>I uptake. *In vivo* administration of MV-NIS either locally or systemically (total dose of  $9 \times 10^6$  TCID<sub>50</sub>) resulted in significant tumor regression ( $P < 0.05$ ) and prolongation of survival ( $P < 0.01$ ). Administration of <sup>131</sup>I further enhanced the antitumor effect of MV-NIS virotherapy ( $P < 0.05$ ). In conclusion, MV-NIS is an oncolytic vector with significant antitumor activity against prostate cancer, which can be further enhanced by <sup>131</sup>I administration. The NIS transgene allows viral localization and monitoring by noninvasive imaging which can facilitate dose optimization in a clinical setting.

### INTRODUCTION

Prostate cancer is the most frequent malignancy in men and the second-leading cause of cancer-related death among men in the USA, with 186,320 new cases and 28,660 prostate cancer-related deaths estimated in 2008.<sup>1</sup> There is currently no cure for metastatic prostate cancer and therefore novel therapeutic strategies are urgently needed. Measles virus (MV) is a negative-strand RNA paramyxovirus that exerts its cytopathic effect (CPE) by formation of multinucleated cell aggregates (syncytia) via cell–cell fusion. MV vaccine strains are

Correspondence: Evanthia Galanis, Division of Medical Oncology, Mayo Clinic College of Medicine, 200 First Street SW, Rochester, Minnesota, 55905, USA. galanis.evanthia@mayo.edu.

SUPPLEMENTARY MATERIAL  
Materials and Methods.

exceptionally harmless and have been safely administered to millions of people with no reversion to pathogenicity or human-to-human transmission documented in over 40 years of use.<sup>2</sup> The attenuated MV Edmonston (MV-Edm) vaccine lineage derivatives have been adapted to enter cells predominantly via the CD46 receptor.<sup>3,4</sup> CD46 is ubiquitously present on primate cells but is frequently overexpressed in tumors, including prostate cancer.<sup>5-9</sup> MV-Edm derivatives can therefore preferentially infect tumor cells causing only minimal CPE in nontransformed tissues.<sup>10-13</sup>

We have previously demonstrated that a recombinant MV-Edm strain engineered to express the human carcinoembryonic antigen (CEA; MV-CEA virus) has potent antitumor activity against prostate cancer cell lines and xenografts.<sup>14</sup> One potential limitation of MV-CEA as a prostate cancer therapeutic is the fact that CEA levels have been found to be moderately elevated in ~1/3 of newly diagnosed prostate cancer patients,<sup>15</sup> thus making difficult the distinction between CEA expression due to viral replication or due to the disease itself. We thus, chose to evaluate the oncolytic potency of a recombinant MV-Edm strain expressing the human sodium iodide symporter (NIS; MV-NIS virus)(Figure 1a),<sup>16</sup> a virus currently being tested in phase I clinical trials against multiple myeloma and ovarian cancer.<sup>17</sup> NIS expression in infected cells following viral replication allows uptake of radioisotopes such as <sup>123</sup>I and <sup>99m</sup>Tc and imaging of viral spread by  $\gamma$ -camera, single photon emission computed tomography or positron emission tomography/computed tomography.<sup>16,18,19</sup> In addition, the therapeutic efficacy of MV-NIS can be increased by combination with <sup>131</sup>I, a  $\beta$ -particle emitter with an average tissue-path length of ~0.8 mm<sup>20</sup> that can elicit a bystander cell-killing effect in neighboring uninfected cells as well as eradicate tumors that are otherwise refractory to oncolysis by MV-NIS itself.<sup>16</sup>

In the present study, we demonstrated that MV-NIS has significant *in vitro* and *in vivo* oncolytic activity against prostate cancer. Increased radioiodide uptake by MV-NIS-infected cells allowed viral localization and monitoring by noninvasive imaging using <sup>123</sup>I. The *in vivo* oncolytic effect of MV-NIS was further enhanced by combination with <sup>131</sup>I (radiovirotherapy) following either intratumoral (IT) or intravenous (IV) injection of the virus. This approach has promising translational potential in prostate cancer treatment.

## RESULTS

### **MV-NIS efficiently replicates in prostate cancer cell lines; NIS expression significantly increases intracellular <sup>125</sup>I concentration**

All three prostate cancer cell lines tested (PC-3, DU-145, and LNCaP) supported robust replication of MV-NIS (Figure 1b). The virus also demonstrated significant *in vitro* oncolytic activity against prostate cancer. The characteristic measles-induced syncytia were apparent by day 2 following MV-NIS infection. As shown in Figure 1c, all three prostate cancer lines were susceptible to MV-NIS-mediated oncolysis with <10% of cells being viable by day 7 post-MV-NIS infection at an multiplicity of infection (MOI) of 1.0. Notably, complete lysis of LNCaP monolayers could be achieved by day 7 using MOIs as low as 0.01. Infected prostate cancer cells were able to effectively concentrate the iodide isotope <sup>125</sup>I indicating the presence of functional NIS on the cell surface (Figure 1d). Cotreatment with potassium perchlorate, a NIS-specific inhibitor, blocked this uptake.

### **MV-NIS efficiently and persistently infects prostate cancer xenografts**

Mice harboring LNCaP xenografts received a single IT or IV injection of MV-NIS or UV-inactivated virus and tumors were harvested on days 3, 8, and 14 post-treatment. Tumors were stained with H&E and examined by *in situ* hybridization for the presence of MV N mRNA, indicating replication. Numerous syncytia were visible in tumors treated with MV-

NIS (Figure 2a). *In situ* hybridization was strongly positive for MV-NIS N mRNA up to at least 14 days following IT or IV administration of the virus (Figure 2b). These results demonstrate that MV-NIS can efficiently infect and propagate in LNCaP prostate cancer xenografts with ongoing viral replication for at least 2 weeks following treatment.

### **MV-NIS transgene expression allows noninvasive imaging of infected tumors *in vivo***

To assess the *in vivo* NIS transgene expression in MV-NIS-treated prostate tumors, MV-NIS was administered IT or IV in mice engrafted with subcutaneous LNCaP xenografts. Mice receiving MV-CEA IT or IV served as controls. Whole-body imaging 1 hour after intraperitoneal injection of  $^{123}\text{I}$  [500  $\mu\text{Ci}$  (18.5 MBq)] was performed to evaluate radioiodide biodistribution at different days following virus treatment. As shown in Figures 3 and 4, significant radioiodide uptake was observed in MV-NIS-infected tumors allowing for localization and monitoring of viral gene expression. Radioiodide uptake was also seen in the thyroid and stomach which normally express NIS.<sup>21</sup> Furthermore,  $^{123}\text{I}$  signal was also detectable in the bladder due to the renal elimination of the isotope. Peak tumor uptake was observed on day 4 in IT- and on day 14 in IV-treated animals. MV-CEA-treated tumors and UV-inactivated MV-NIS-treated tumors did not concentrate  $^{123}\text{I}$  (data not shown). Quantitative analysis of  $^{123}\text{I}$  absorption by MV-NIS-infected tumors showed strong radioisotope accumulation and retention over time both in IT- and IV-treated animals (Figures 3c,d). Figure 4 illustrates the ability of the NIS transgene to monitor the sites of *MV-NIS* gene expression over time. Persistent transgene expression could be identified for as long as 36 days following IV administration of the virus.

### **MV-NIS has potent antitumor activity when administered IT or IV even at low doses in nude mice bearing prostate cancer xenografts**

The *in vivo* oncolytic potency of MV-NIS was assessed in established subcutaneous LNCaP xenografts. All mice treated with six injections of MV-NIS either IT or IV had significant suppression of tumor growth ( $P < 0.05$ ) by day 23 compared to mice treated with UV-inactivated MV-NIS. Tumors treated with a single injection of MV-NIS did not differ significantly in size as compared to the controls at the time of death of the first control mice (day 23 post-treatment initiation). However, as shown in Figure 5, even this low dose treatment ultimately caused partial regressions and slowed tumor progression long enough to produce a survival benefit. Thus, mice treated with a single MV-NIS dose either IT or IV had significantly longer survival compared to the UV-inactivated controls ( $P < 0.05$ ). Notably, all mice treated with six injections of MV-NIS were alive by day 120 post-treatment initiation (Figure 5). This dosing schedule resulted in remarkable regression of these relatively large tumors with 4/5 mice in each of these two groups (IT and IV MV-NIS administration) accomplishing complete tumor regression. Interestingly, the two administration routes showed different initial kinetics. Tumor regression in the IV group lagged by ~10 days as compared to the IT group. Rapid oncolysis in the IV group was observed starting at ~14 days post-treatment initiation, and resulted in equivalent tumor regression to the IT group by day 17. This effect strongly corresponded to the different viral kinetics observed by  $^{123}\text{I}$  imaging (Figures 3 and 4). As Figure 4 illustrates, there was limited initial infection following IV MV-NIS administration that by day 14 has markedly expanded into the whole tumor mass. Each of the two mice serially imaged in Figure 4 over a period of 48 days exhibited a distinct biological response to IV MV-NIS treatment that correlated with the results of  $^{123}\text{I}$  imaging. More specifically, single dose MV-NIS administration in mouse A resulted in significant regression of the tumor that was evident at 19 days post-treatment. By day 36, the tumor had shrunk to <25% of its original volume and viral infection was undetectable by  $^{123}\text{I}$  imaging, with the tumor eventually relapsing. On the other hand, mouse B exhibited primarily tumor growth arrest (stable disease) effectuated

by the underlying MV-NIS infection which was persistently strong even at 36 days post-treatment.

### Radiovirotherapy with $^{131}\text{I}$ enhances the oncolytic effect of MV-NIS in prostate cancer xenografts

To determine the potential therapeutic benefit of MV-NIS-mediated radiovirotherapy using  $^{131}\text{I}$  in prostate cancer tumors, we administered a single dose of MV-NIS either IT or IV and measured radioiodide retention time in infected LNCaP xenografts at the respective day of peak isotope uptake (day 4 and day 14 post-MV-NIS treatment). Dosimetric calculations were performed as described in the **Supplementary Materials and Methods**. Based on the *in vivo* uptake curves of  $^{131}\text{I}$  (Figures 3c,d) we calculated the absorbed tumor dose of radiovirotherapy with  $^{131}\text{I}$  to be at least 400 cGy (an average of 420 or 540 cGy when MV-NIS was administered IT or IV respectively) using a dose of 1,000  $\mu\text{Ci}$  (37 MBq)  $^{131}\text{I}$ .

Figure 6 illustrates the impact of radiovirotherapy on mice bearing subcutaneous LNCaP xenografts. Even at a low total viral dosage of  $1.5 \times 10^6$  TCID<sub>50</sub>/mouse, a statistically significant suppression of tumor growth ( $P < 0.05$ ) was observed in the combined radiovirotherapy group by day 25 post IT MV-NIS injection (Figure 6a) and day 27 post IV MV-NIS injection (Figure 6b). Single-agent MV-NIS therapy IT or IV significantly prolonged survival compared to the UV-inactivated control groups (Figures 6c,d;  $P < 0.05$ ). However, combination with  $^{131}\text{I}$  resulted in a statistically significant prolongation of survival compared to the single-agent MV-NIS-treated groups ( $P < 0.05$ ). We did not observe any  $^{131}\text{I}$ -related toxicity with the exception of one animal in the combined radiovirotherapy group which developed mild acute lower intestinal bleeding. This mouse fully responded to radiovirotherapy, became tumor-free and remained healthy until the experiment was terminated on day 120. Similarly, three mice in the IV radiovirotherapy group showed complete tumor regression and no  $^{131}\text{I}$ -related toxicity was observed.

## DISCUSSION

This study demonstrated that MV-NIS has considerable oncolytic activity against prostate cancer cell lines and xenografts when administered IT or IV. Of note, both androgen-sensitive (LNCaP) and -insensitive (PC-3 and DU-145) lines were susceptible to the CPE of MV-NIS and supported robust viral replication (Figure 1). We have previously reported on the antitumor activity of a different MV-Edm strain (MV-CEA) in PC-3 xenografts.<sup>14</sup> In the present study, we established the efficacy of MV derivatives, MV-NIS in particular, in a second animal model of prostate cancer. Thus, athymic nude mice bearing subcutaneous LNCaP xenografts received IT or IV injections of MV-NIS. The virus successfully and persistently infected the tumors. Histological slides revealed the characteristic CPE of MV-NIS *in vivo* (Figure 2). *In situ* hybridization for MV-NIS N mRNA further confirmed the presence of replicating virus in tumor tissue for at least 2 weeks following treatment. NIS-mediated noninvasive imaging of  $^{123}\text{I}$  absorption facilitated analysis and interpretation of the different oncolytic behavior of MV-NIS in individual animals (Figure 4), and confirmed transgene expression for up to 36 days following IV viral administration. Therefore, monitoring of virus-driven NIS expression is a safe, noninvasive approach that can address questions pertaining to the oncolytic virus activity in cancer patients, and thus facilitate dose optimization and development of individualized therapeutic protocols. In addition, quantitation of radioiodide uptake by NIS imaging can provide important dosimetric information on the optimal dosing for MV-NIS-mediated  $^{131}\text{I}$  therapy.

It should be noted that our *in vivo* imaging data showing viral persistence for >4 weeks in prostate cancer xenografts were obtained in immune deficient athymic nude mice, lacking

adaptive immune function. In humans, systemic antiviral immunity can decrease the antitumor activity of the virus, especially following systemic administration, nevertheless the impact of systemic immune response following IT administration is less significant. In addition, however, a key component of MV persistence in infected tumors is the innate immune response.<sup>22</sup> Therefore, the fact that our data were generated in a mouse model that maintains innate immunity, including macrophage and NK cell activity<sup>23,24</sup> is encouraging.

Our standard treatment schedule of six recombinant MV-Edm doses resulted in complete elimination of the tumors by MV-NIS in 80% of mice bearing prostate cancer LNCaP xenografts regardless of the route of administration employed. Notably, all treated mice were alive at the end of this experiment (day 120 post-treatment initiation). Despite this very encouraging survival data following repeat viral administration, we decided to also test subtherapeutic doses of MV-NIS, either alone or in combination with <sup>131</sup>I. The results obtained in this setting emphasize that even in an unfavorable virus particle/tumor cell ratio, as for example, might be expected in a heavy tumor burden clinical scenario, we can observe significant oncolytic activity which can be further augmented by radiovirotherapy with <sup>131</sup>I. Thus, a single dose of MV-NIS significantly prolonged survival of mice engrafted with subcutaneous LNCaP xenografts ( $P < 0.05$ ) but this relatively small dose was not able to completely eradicate the tumors alone (Figure 5). However, a single injection of MV-NIS combined with <sup>131</sup>I was able to completely eradicate 40–60% of the tumors and significantly prolonged survival as compared to single-agent MV-NIS therapy ( $P < 0.05$ ).

MV-NIS is an attenuated measles vaccine derivative. Measles vaccine strains have been shown to lack significant CPE in non-malignant cells including normal ovarian surface epithelial cells, astrocytes, mesothelial cells, hepatocytes, peripheral blood lymphocytes, and coronary artery smooth muscle cells.<sup>10–13</sup> As expression of the measles receptor CD46 has been previously detected in prostate tissues<sup>7</sup> and in order to address safety considerations, a pilot toxicology study of intraprostatic administration of highly concentrated MV-NIS has been performed and will be reported separately (P. Msaouel and E. Galanis, unpublished results). *Ifnar*<sup>ko</sup> CD46 Ge mice, a transgenic mouse strain that is very sensitive to MV-Edm infection and has been used for toxicology assessment of oncolytic MV-Edm strains,<sup>25–28</sup> have been employed in this pilot study. The dose of MV-NIS injected into the transgenic animal prostate corresponded to a dose of  $\sim 3 \times 10^9$  TCID<sub>50</sub> in an average-sized human prostate<sup>29</sup> and was thus higher than maximum doses administered in currently ongoing clinical trials of MV-NIS. No significant MV-NIS-related clinical or pathological toxicity was observed pointing to the safety and tolerability of this approach.

There has been a recent resurgence in oncolytic virotherapy research and prostate cancer was quickly recognized as a promising candidate for these approaches. Translational attempts have up to now mostly focused on replicating oncolytic adenoviral vectors and early evidence of biologic activity in patients has been reported.<sup>30–34</sup> Notably, a recent report indicated the feasibility of noninvasive imaging in prostate cancer patients using the *NIS* reporter gene following IT administration of a replication-competent adenovirus carrying two suicide genes and the *NIS* gene.<sup>35</sup> These adenoviruses target cells via the coxsackievirus adenovirus receptor which exhibits variable expression during the different stages of disease progression.<sup>36</sup> On the other hand, the measles receptor CD46 shows consistently strong expression in prostate lines and tumors.<sup>5–7,14</sup> Furthermore, MV-Edm strains exhibit potent bystander killing mediated by massive cell–cell fusion which can destroy noninfected tumor cells. Direct cell-to-cell propagation via fusion can also considerably protect the virus from antibody-mediated neutralization.<sup>37</sup> These properties make MV-NIS an excellent candidate for translation in clinical trials for recurrent prostate cancer patients. Of note, the virus is already in clinical testing for two other indications: as

an IV therapy for multiple myeloma patients, and following intraperitoneal administration in ovarian cancer patients.<sup>17</sup>

Although previous reports have documented the ablative effects of <sup>131</sup>I following nonreplicating virus-mediated human NIS transfer in prostate cancer xenografts,<sup>38</sup> the present study is the first to demonstrate an enhanced antitumor effect against prostate cancer by a replication-competent oncolytic virus carrying the *NIS* gene. A replication-defective adenovirus expressing NIS under the control of CMV promoter (Ad5CMV-NIS) has been developed in our institution and is currently being tested in patients with locally recurrent prostate cancer (J.C. Morris, unpublished results). This trial utilizes NIS both as an imaging and a therapeutic transgene and the data accumulated will be important in designing a future trial of MV-NIS radiovirotherapy against prostate cancer. Although the antitumor activity of Ad5CMV-NIS depends solely on NIS transgene activity, our current approach capitalizes on the already potent oncolytic properties of replicating MV-Edm derivatives. Thus, significant enhancement of MV-NIS antitumor activity could be accomplished using ~1/3 of the <sup>131</sup>I dose previously required, when Ad5CMV-NIS was employed in preclinical experiments.<sup>38</sup>

In summary, we have demonstrated that MV-NIS can successfully infect and destroy prostate cancer tumors when administered either locally or systemically. The potent oncolytic activity of the virus against prostate tumors can be further enhanced by coadministration of <sup>131</sup>I. Virus localization and spread can be non-invasively monitored by <sup>123</sup>I imaging. Our results pave the way for a clinical trial using engineered measles strains against prostate cancer.

## MATERIALS AND METHODS

### Cell lines

Vero (African green monkey) cell line and human prostate cancer cell lines PC-3, DU-145, and LNCaP were purchased from American Type Culture Collection (ATCC, Manassas, VA). All cell lines were grown at 37 °C in media recommended by ATCC in a humidified atmosphere of 5% CO<sub>2</sub>. All media contained 100 U/ml penicillin-streptomycin and were supplemented with 10% heat-inactivated fetal bovine serum.

### Viruses

The construction of recombinant MV-Edm encoding the human NIS protein (MV-NIS) has been described elsewhere.<sup>16</sup> In summary, a complementary DNA infectious clone derived from the Edmonston vaccine lineage Seed B<sup>39</sup> was engineered by inserting the human *NIS* gene downstream from the MV hemagglutinin (*H*) gene (Figure 1a). MV-Edm encoding the soluble extracellular domain of human CEA (MV-CEA) was generated as previously described by inserting the *CEA* gene upstream of the nucleoprotein (*N*) gene.<sup>40</sup> The viruses were propagated by infecting  $1.5 \times 10^6$  Vero cells in T75 flasks at a MOI of 0.02 in 3 ml Opti-MEM (Invitrogen, Carlsbad, CA) at 37 °C for 2 hours. The medium was then replaced with Dulbecco's modified Eagle's medium. The cells were incubated at 37 °C for 2 days and then transferred to 32 °C for 1 day, and subsequently harvested in 1 ml Opti-MEM. The viruses were then released by two cycles of freezing and thawing. The titers of viral stocks were determined by 50% end-point dilution assays (TCID<sub>50</sub>) on Vero cells in 96-well plates.

Preparations of inactivated viruses followed the same procedures as described above. The viruses were inactivated by exposure to UV light at 120,000 μJ/cm<sup>2</sup> for 90 minutes. Viral inactivation was confirmed by titration on Vero cells.

### Assessment of MV-NIS CPE *in vitro*

Cell viability was determined using the cell proliferation kit I (MTT) colorimetric assay. PC-3, DU-145, and LNCaP cells were plated at a density of  $10^4$  cells/well in 96-well plates. Twenty-four hours after seeding, the cells were infected with MV-NIS at different MOIs (0.1, 1, and 10) in 1 ml of Opti-MEM for 2 hours at 37 °C. At the end of the incubation period, the virus was removed and the cells were maintained in their standard medium. Cell proliferation kit I assays (ATCC) were performed at 48, 96, and 168 hours after infection following the manufacturer's instructions. Briefly, cells were incubated with 10% cell proliferation kit I added directly to the medium for 4 hours at 37 °C, followed by cell lysis with a detergent reagent (ATCC) overnight in the dark at room temperature. Absorbance was determined in a SpectraMax microplate reader (Molecular Devices, Sunnyvale, CA) at 570 nm in six different wells per group and results were calculated as the percent of optical density in the infected wells versus the uninfected controls. Vero cells were used as positive controls in each experiment. Results are presented as the means of three independent experiments  $\pm$  SEM.

### Assessment of MV-NIS replication in prostate cancer cell lines

PC-3, DU-145, and LNCaP cells were plated in six-well plates at a density of  $2 \times 10^5$  cells/well. Twenty-four hours after seeding, the cells were infected with MV-NIS at a MOI of 1.0 in 1 ml of Opti-MEM for 2 hours at 37 °C. At the end of the incubation period, the virus was removed and the cells were maintained in their standard medium. The cells were harvested at 24, 48, and 72 hours from two different wells per time point and MV-NIS was released by two cycles of freezing/thawing. The viral titer at each well was determined by 50% end-point dilution assay (TCID<sub>50</sub>) on Vero cells in a 96-well plate. Results are presented as the means of three independent experiments  $\pm$  SEM.

### *In vitro* iodide uptake assay

*In vitro* <sup>125</sup>I uptake of MV-NIS-infected prostate cancer cells was determined at steady-state conditions at 24, 48, and 72 hours after infection as previously described<sup>41</sup> and detailed in the **Supplementary Materials and Methods**.

### Animal experiments

All experimental protocols were approved by the Mayo Foundation Institutional Animal Care and Use Committee.

### Subcutaneous LNCaP tumor model

Xenografts derived from the LNCaP cell line were established into the right flanks of 6–8-week-old male BALB/c nude mice by subcutaneous injection of  $5 \times 10^6$  cells suspended in 0.1 ml phosphate-buffered saline and 0.1 ml of BD Matrigel basement membrane matrix (BD Biosciences, Bedford, MA). The mice were examined daily for tumor growth. All mice received levothyroxine (5 mg/ml) in their drinking water to suppress thyroidal NIS expression.<sup>38</sup> Tumor volume was measured with calipers twice weekly and calculated by the formula: volume = [(smallest diameter)<sup>2</sup> × (largest diameter)]/2. Tumor volumes were measured by calipers twice per week. The mice were euthanized if the tumor volume was  $>2,000$  mm<sup>3</sup>, if tumor ulcerations developed or if weight loss  $>20\%$  of body weight was observed.

Histological assessment and *in situ* hybridization for MV-NIS N mRNA were performed as described in the **Supplementary Materials and Methods**.

### ***In vivo* $^{123}\text{I}$ imaging and dosimetry**

Mice were subcutaneously engrafted with LNCaP cells as described above. When all tumors reached  $100\text{ mm}^3$ , mice received one IT or IV injection of either  $1.5 \times 10^6$  TCID<sub>50</sub> MV-NIS or the same dose of MV-CEA ( $n = 3$  mice per group). Mice were injected with  $^{123}\text{I}$  [500  $\mu\text{Ci}$  (18.5 MBq)] intraperitoneally and imaged using a micro- $\gamma$  camera system (Gamma Medica, Northridge, CA) on days 1, 4, 5, 8, and 11 following IT virus administration or days 1, 4, 5, 8, and 11, 14, and 18 following IV virus injection. Tumor activity was measured by region of interest image analysis using the PMOD Biomedical Imaging Quantification and Kinetic Modelling Software (PMOD Technologies, Zurich, Switzerland).

To determine the radiation dose absorbed by MV-NIS-infected tumors, a single dose of MV-NIS was administered IT or IV ( $n = 3$  per group). Tumor dosimetry was performed at the respective day of peak isotope uptake (day 4 and day 14) by serial imaging of mice at 1, 3, 6, 9, 12, and 24 hours after receiving a single injection of  $^{123}\text{I}$  as described in the **Supplementary Materials and Methods**.

### **Assessment of *in vivo* efficacy of IT or IV MV-NIS Treatment**

Male BALB/c nude mice were subcutaneously engrafted with LNCaP cells as described above. Virus injection was initiated ~3–4 weeks after tumor cell implantation when all tumor volumes were  $>100\text{ mm}^3$ . The first experiment assessed the efficacy of MV-NIS administration ( $1.5 \times 10^6$  TCID<sub>50</sub> in 100  $\mu\text{l}$  Opti-MEM) via the IT and the IV route of administration and compared the effect of 1 versus 6 doses ( $1.5 \times 10^6$  TCID<sub>50</sub> in 100  $\mu\text{l}$  Opti-MEM each, administered twice weekly for a total dose of  $9 \times 10^6$  TCID<sub>50</sub>). Thus, mice were assigned into one of eight groups (five mice each): IT administration of MV-NIS (one injection), IT administrations of MV-NIS (six injections), IT administration of UV-inactivated MV-NIS (one injection), IT administrations of UV-inactivated MV-NIS (six injections), IV administration of MV-NIS (one injection), IV administrations of MV-NIS (six injections), IV administration of UV-inactivated MV-NIS (one injection), IV administrations of UV-inactivated MV-NIS (six injections).

### **Assessment of *in vivo* efficacy of IT or IV MV-NIS-mediated radiovirotherapy**

To evaluate the therapeutic benefit of radiovirotherapy in this setting, eight groups of mice ( $n = 5$  per group) with established subcutaneous LNCaP tumors (all  $>100\text{ mm}^3$ ) were treated IT or IV with a single injection of MV-NIS ( $1.5 \times 10^6$  TCID<sub>50</sub> in 100  $\mu\text{l}$  Opti-MEM) or an equivalent dose of UV-inactivated virus with or without subsequent  $^{131}\text{I}$  administration [1 mCi (37 MBq) per mouse injected intraperitoneally]. The optimal timing for therapeutic administration of  $^{131}\text{I}$  corresponded to the time-point of maximal radioiodide uptake, as determined by the  $^{123}\text{I}$  imaging data. Thus,  $^{131}\text{I}$  was intraperitoneally administered on day 4 in the IT group and day 14 in the IV-treatment group. Control mice that did not receive  $^{131}\text{I}$  were injected with an equal volume of normal saline (0.9% solution) intraperitoneally at the corresponding time points.

### **Statistical analysis**

Statistical analysis was performed with the GraphPad Prism 5.0 software (GraphPad Software, San Diego, CA). Tumor volume differences between two groups were assessed using the Mann–Whitney *U*-test. Survival curves were plotted according to the Kaplan–Meier method. The logrank test was used to compare the survival times of the two *in vivo* treatment groups. A  $P \leq 0.05$  was considered statistically significant.



## Acknowledgments

We acknowledge Teresa D. Decklever for excellent technical assistance with the radioiodide imaging and Alan R. Penheiter for helpful discussions. We also thank the members of the Mayo Clinic Viral Vector Production Laboratory: Linda Gregory, Guy Griesmann, Kirsten Langfield, Julie Sauer, Sharon Stephan, Henry Walker, Troy Wegman, and Cindy Whitcomb. Finally, we thank Raquel Ostby for help with manuscript preparation. This study was supported by the Mayo Clinic Prostate SPORE grant P50 CA 091956 (E.G., P.M., J.C.M.).

## References

1. Jemal A, Siegel R, Ward E, Hao Y, Xu J, Murray T, et al. Cancer statistics. *CA Cancer J Clin* 2008;58:71–96. [PubMed: 18287387]
2. Griffin DE, Pan CH, Moss WJ. Measles vaccines. *Front Biosci* 2008;13:1352–1370. [PubMed: 17981635]
3. Dörig RE, Marcil A, Chopra A, Richardson CD. The human CD46 molecule is a receptor for measles virus (Edmonston strain). *Cell* 1993;75:295–305. [PubMed: 8402913]
4. Nanche D, Varior-Krishnan G, Cervoni F, Wild TF, Rossi B, Rabourdin-Combe C, et al. Human membrane cofactor protein (CD46) acts as a cellular receptor for measles virus. *J Virol* 1993;67:6025–6032. [PubMed: 8371352]
5. Buettner R, Huang M, Gritsko T, Karras J, Enkemann S, Mesa T, et al. Activated signal transducers and activators of transcription 3 signaling induces CD46 expression and protects human cancer cells from complement-dependent cytotoxicity. *Mol Cancer Res* 2007;5:823–832. [PubMed: 17699108]
6. Liu AY. Differential expression of cell surface molecules in prostate cancer cells. *Cancer Res* 2000;60:3429–3434. [PubMed: 10910052]
7. Loberg RD, Wojno KJ, Day LL, Pienta KJ. Analysis of membrane-bound complement regulatory proteins in prostate cancer. *Urology* 2005;66:1321–1326. [PubMed: 16360477]
8. Baczko K, Lazzarini RA. Efficient propagation of measles virus in suspension cultures. *J Virol* 1979;31:854–855. [PubMed: 513197]
9. Fishelson Z, Donin N, Zell S, Schultz S, Kirschfink M. Obstacles to cancer immunotherapy: expression of membrane complement regulatory proteins (mCRPs) in tumors. *Mol Immunol* 2003;40:109–123. [PubMed: 12914817]
10. Anderson BD, Nakamura T, Russell SJ, Peng KW. High CD46 receptor density determines preferential killing of tumor cells by oncolytic measles virus. *Cancer Res* 2004;64:4919–4926. [PubMed: 15256464]
11. Blechacz B, Splinter PL, Greiner S, Myers R, Peng KW, Federspiel MJ, et al. Engineered measles virus as a novel oncolytic viral therapy system for hepatocellular carcinoma. *Hepatology* 2006;44:1465–1477. [PubMed: 17133484]
12. Peng KW, Donovan KA, Schneider U, Cattaneo R, Lust JA, Russell SJ. Oncolytic measles viruses displaying a single-chain antibody against CD38, a myeloma cell marker. *Blood* 2003;101:2557–2562. [PubMed: 12433686]
13. Phuong LK, Allen C, Peng KW, Giannini C, Greiner S, TenEyck CJ, et al. Use of a vaccine strain of measles virus genetically engineered to produce carcinoembryonic antigen as a novel therapeutic agent against glioblastoma multiforme. *Cancer Res* 2003;63:2462–2469. [PubMed: 12750267]
14. Msaouel P, Iankov ID, Allen C, Morris JC, von Messling V, Cattaneo R, et al. Engineered measles virus as a novel oncolytic therapy against prostate cancer. *Prostate* 2009;69:82–91. [PubMed: 18973133]
15. Neufeld L, Dubin A, Guinan P, Nabong R, Ablin RJ, Bush IM. Carcinoembryonic antigen in the diagnosis of prostate carcinoma. *Oncology* 1974;29:376–381. [PubMed: 4850875]
16. Dingli D, Peng KW, Harvey ME, Greipp PR, O'Connor MK, Cattaneo R, et al. Image-guided radiovirotherapy for multiple myeloma using a recombinant measles virus expressing the thyroidal sodium iodide symporter. *Blood* 2004;103:1641–1646. [PubMed: 14604966]
17. Msaouel P, Dispenzieri A, Galanis E. Clinical testing of engineered oncolytic measles virus strains in the treatment of cancer: an overview. *Curr Opin Mol Ther* 2009;11:43–53. [PubMed: 19169959]

18. Spitzweg C, O'Connor MK, Bergert ER, Tindall DJ, Young CY, Morris JC. Treatment of prostate cancer by radioiodine therapy after tissue-specific expression of the sodium iodide symporter. *Cancer Res* 2000;60:6526–6530. [PubMed: 11103823]
19. Dingli D, Kemp BJ, O'Connor MK, Morris JC, Russell SJ, Lowe VJ. Combined I-124 positron emission tomography/computed tomography imaging of NIS gene expression in animal models of stably transfected and intravenously transfected tumor. *Mol Imaging Biol* 2006;8:16–23. [PubMed: 16328647]
20. Dingli D, Russell SJ, Morris JC. *In vivo* imaging and tumor therapy with the sodium iodide symporter. *J Cell Biochem* 2003;90:1079–1086. [PubMed: 14635183]
21. Zuckier LS, Dohan O, Li Y, Chang CJ, Carrasco N, Dadachova E, et al. Kinetics of perhenate uptake and comparative biodistribution of perhenate, pertechnetate, and iodide by NaI symporter-expressing tissues *in vivo*. *J Nucl Med* 2004;45:500–507. [PubMed: 15001694]
22. Griffin, DE. Measles virus. In: Knipe, DM.; Howley, PM., editors. *Fields' Virology*. Wolters Kluwer/Lippincott Williams & Wilkins; Philadelphia, PA; London: 2001. p. 1401-1442.
23. Tsutsui H, Nakanishi K, Matsui K, Higashino K, Okamura H, Miyazawa Y, et al. IFN-gamma-inducing factor up-regulates Fas ligand-mediated cytotoxic activity of murine natural killer cell clones. *J Immunol* 1996;157:3967–3973. [PubMed: 8892629]
24. Hooijberg E, van den Berk PC, Sein JJ, Wijdenes J, Hart AA, de Boer RW, et al. Enhanced antitumor effects of CD20 over CD19 monoclonal antibodies in a nude mouse xenograft model. *Cancer Res* 1995;55:840–846. [PubMed: 7531616]
25. Mrkic B, Odermatt B, Klein MA, Billeter MA, Pavlovic J, Cattaneo R. Lymphatic dissemination and comparative pathology of recombinant measles viruses in genetically modified mice. *J Virol* 2000;74:1364–1372. [PubMed: 10627547]
26. Mrkic B, Pavlovic J, Rüllicke T, Volpe P, Buchholz CJ, Hourcade D, et al. Measles virus spread and pathogenesis in genetically modified mice. *J Virol* 1998;72:7420–7427. [PubMed: 9696838]
27. Roscic-Mrkic B, Schwendener RA, Odermatt B, Zuniga A, Pavlovic J, Billeter MA, et al. Roles of macrophages in measles virus infection of genetically modified mice. *J Virol* 2001;75:3343–3351. [PubMed: 11238860]
28. Kemper C, Leung M, Stephensen CB, Pinkert CA, Liszewski MK, Cattaneo R, et al. Membrane cofactor protein (MCP; CD46) expression in transgenic mice. *Clin Exp Immunol* 2001;124:180–189. [PubMed: 11422193]
29. Freedland SJ, Platz EA, Presti JC, Aronson WJ, Amling CL, Kane CJ, et al. Obesity, serum prostate specific antigen and prostate size: implications for prostate cancer detection. *J Urol* 2006;175:500–4. discussion 504. [PubMed: 16406980]
30. DeWeese TL, van der Poel H, Li S, Mikhak B, Drew R, Goemann M, et al. A phase I trial of CV706, a replication-competent, PSA selective oncolytic adenovirus, for the treatment of locally recurrent prostate cancer following radiation therapy. *Cancer Res* 2001;61:7464–7472. [PubMed: 11606381]
31. Small EJ, Carducci MA, Burke JM, Rodriguez R, Fong L, van Ummersen L, et al. A phase I trial of intravenous CG7870, a replication-selective, prostate-specific antigen-targeted oncolytic adenovirus, for the treatment of hormone-refractory, metastatic prostate cancer. *Mol Ther* 2006;14:107–117. [PubMed: 16690359]
32. Freytag SO, Khil M, Stricker H, Peabody J, Menon M, DePeralta-Venturina M, et al. Phase I study of replication-competent adenovirus-mediated double suicide gene therapy for the treatment of locally recurrent prostate cancer. *Cancer Res* 2002;62:4968–4976. [PubMed: 12208748]
33. Freytag SO, Movsas B, Aref I, Stricker H, Peabody J, Pegg J, et al. Phase I trial of replication-competent adenovirus-mediated suicide gene therapy combined with IMRT for prostate cancer. *Mol Ther* 2007;15:1016–1023. [PubMed: 17375076]
34. Freytag SO, Stricker H, Pegg J, Paielli D, Pradhan DG, Peabody J, et al. Phase I study of replication-competent adenovirus-mediated double-suicide gene therapy in combination with conventional-dose three-dimensional conformal radiation therapy for the treatment of newly diagnosed, intermediate- to high-risk prostate cancer. *Cancer Res* 2003;63:7497–7506. [PubMed: 14612551]

35. Barton KN, Stricker H, Brown SL, Elshaikh M, Aref I, Lu M, et al. Phase I study of noninvasive imaging of adenovirus-mediated gene expression in the human prostate. *Mol Ther* 2008;16:1761–1769. [PubMed: 18714306]
36. Rauen KA, Sudilovsky D, Le JL, Chew KL, Hann B, Weinberg V, et al. Expression of the coxsackie adenovirus receptor in normal prostate and in primary and metastatic prostate carcinoma: potential relevance to gene therapy. *Cancer Res* 2002;62:3812–3818. [PubMed: 12097294]
37. Iankov ID, Blechacz B, Liu C, Schmeckpeper JD, Tarara JE, Federspiel MJ, et al. Infected cell carriers: a new strategy for systemic delivery of oncolytic measles viruses in cancer virotherapy. *Mol Ther* 2007;15:114–122. [PubMed: 17164782]
38. Spitzweg C, Dietz AB, O'Connor MK, Bergert ER, Tindall DJ, Young CY, et al. *In vivo* sodium iodide symporter gene therapy of prostate cancer. *Gene Ther* 2001;8:1524–1531. [PubMed: 11704812]
39. Radecke F, Spielhofer P, Schneider H, Kaelin K, Huber M, Dötsch C, et al. Rescue of measles viruses from cloned DNA. *EMBO J* 1995;14:5773–5784. [PubMed: 8846771]
40. Peng KW, Facteau S, Wegman T, O'Kane D, Russell SJ. Non-invasive *in vivo* monitoring of trackable viruses expressing soluble marker peptides. *Nat Med* 2002;8:527–531. [PubMed: 11984600]
41. Weiss SJ, Philp NJ, Grollman EF. Iodide transport in a continuous line of cultured cells from rat thyroid. *Endocrinology* 1984;114:1090–1098. [PubMed: 6705729]

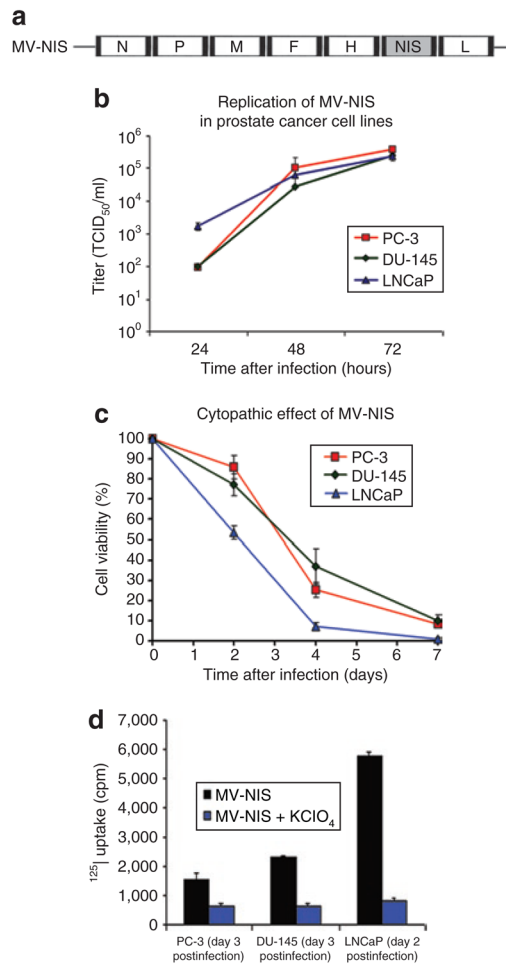


**Figure 1. Replication and cytopathic effect of MV-NIS on prostate cancer cell lines and *in vitro* Iodide-125 ( $^{125}\text{I}$ ) uptake of cells infected with MV-NIS**

(a) Schematic representation of measles virus–sodium iodide symporter (MV-NIS). The complementary DNA encoding for the human thyrocyte sodium iodide symporter (NIS) was inserted downstream of the hemagglutinin (*H*) gene (*N*, nucleoprotein gene; *P*, phosphoprotein gene; *M*, matrix protein gene; *F*, fusion protein gene; *L*, large protein gene). (b) MV-NIS efficiently replicates in PC-3, DU-145, and LNCaP prostate cancer cells as demonstrated by one-step growth curves for cell-associated virus. (c) Cytopathic effect of MV-NIS on PC-3, DU-145, and LNCaP cells at multiplicity of infection (MOI) = 1.0. Cell viability was determined by the cell proliferation kit I (MTT) colorimetric assay. Monolayer cell cultures were completely eradicated by day 7. (d) *In vitro* Iodide-125 ( $^{125}\text{I}$ ) uptake of prostate cancer cells infected with MV-NIS with or without potassium perchlorate ( $\text{KClO}_4$ ). Prostate cancer cell lines were infected with MV-NIS at a MOI of 1.0. Infected cells cocultured with  $\text{KClO}_4$ , a competitive inhibitor of iodide uptake by NIS, were used as controls. Significantly more radioiodide uptake was observed in MV-NIS-infected cells as compared to controls in all prostate cancer cell lines tested ( $P < 0.05$  for all comparisons). Results are presented as the means of three independent experiments  $\pm$  SEM.

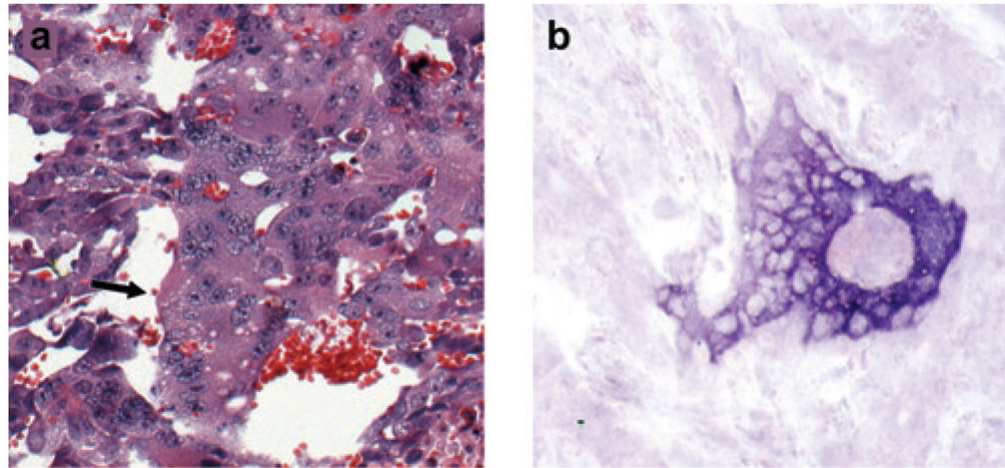


**Figure 2. *In vivo* MV-NIS infection of prostate cancer xenografts**

Histological sections reveal persistent infection and extensive syncytia formation in LNCaP xenografts 14 days after a single intravenous (IV) administration of  $1.5 \times 10^6$  TCID<sub>50</sub> of measles virus–sodium iodide symporter (MV-NIS). (a) Hematoxylin and eosin (H&E) staining of LNCaP tumor 14 days after IV MV-NIS injection. Extensive syncytia formation within the tumor is shown (arrow) (original magnification  $\times 200$ ). (b) *in situ* hybridization for MV-NIS N mRNA confirms viral replication in these tumors (original magnification  $\times 200$ ).

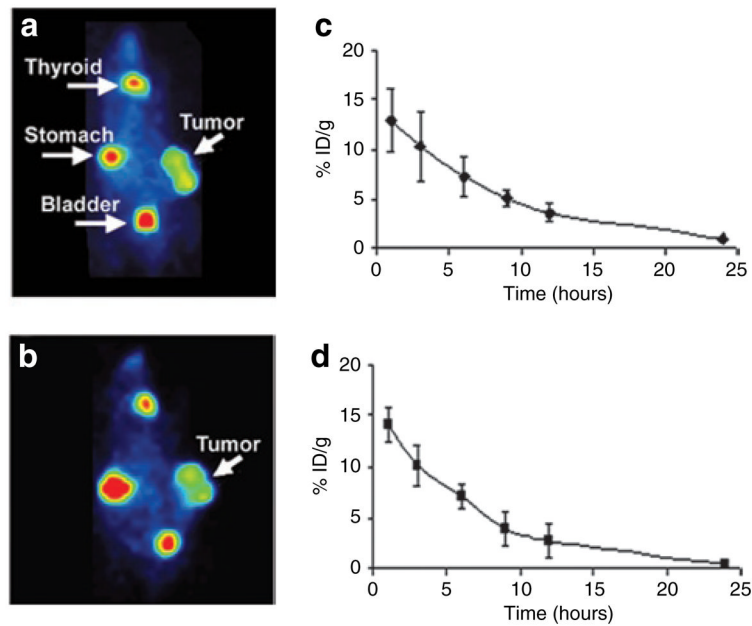


**Figure 3. *In vivo* imaging of prostate cancer tumors infected with MV-NIS**

Mice bearing subcutaneous LNCaP tumor xenografts on their right flank received a single intratumoral (IT) or intravenous (IV) dose of  $1.5 \times 10^6$  TCID<sub>50</sub> of measles virus–sodium iodide symporter (MV-NIS). MV-NIS infection led to strong, localized, functional NIS expression on the prostate cancer cells resulting in significant <sup>123</sup>I uptake. Representative radioiodide images are shown. Strong positive tumor <sup>123</sup>I uptake is seen 4 days after IT administration of MV-NIS (a) or 14 days after IV administration of MV-NIS (b). Quantification of radioiodide uptake showed significant uptake and retention of the isotope in the tumor 4 days after IT injection (c). Similarly, significant <sup>123</sup>I uptake and retention were observed 14 days after IV administration of MV-NIS (d). Error bars in c,d indicate the SD from the mean.

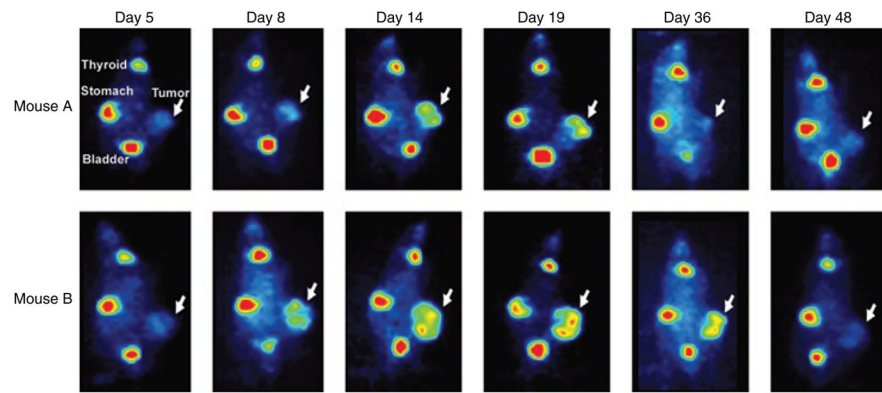


**Figure 4. *In vivo* monitoring of MV-NIS infection over time**

Two mice harboring LNCaP xenografts received a single IV injection of  $1.5 \times 10^6$  TCID<sub>50</sub> measles virus–sodium iodide symporter (MV-NIS) and viral biodistribution and kinetics were monitored by <sup>123</sup>I imaging. Initially, MV-NIS carried by the blood supply into the xenograft could be detected in small, localized sites inside the tumor. By day 14, the replicating virus had spread extensively throughout the tumor mass and strong, persistent infection could be detected for as long as 36 days. MV-NIS replication inside the tumor of mouse A resulted in significant partial regression of the growth that relapsed when the virus was cleared (negative uptake signal). Mouse B exhibited tumor growth arrest (stable disease) due to persistent MV-NIS infection. The virus was ultimately cleared from the mouse and tumor growth was reinstated.

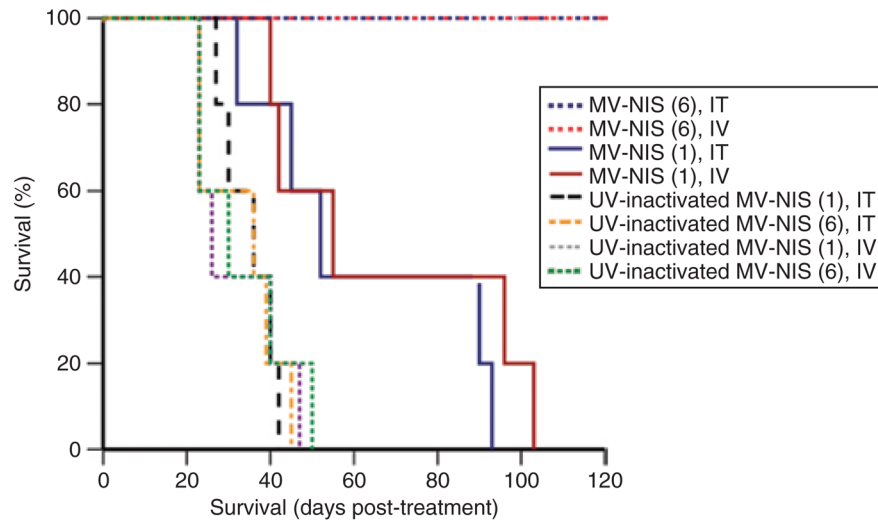


**Figure 5. Oncolytic activity of MV-NIS administered IT or IV in a subcutaneous LNCaP prostate cancer model**

Mice ( $n = 5$  per group) received a single intratumoral (IT) or intravenous (IV) dose of  $1.5 \times 10^6$  TCID<sub>50</sub> measles virus–sodium iodide symporter (MV-NIS) or six injections (IT or IV) of the virus at a total dose of  $9 \times 10^6$  TCID<sub>50</sub> or equivalent control regimens of UV-inactivated MV-NIS. All mice treated with six MV-NIS doses injected either IT or IV were alive by day 120 post-treatment initiation (these two curves completely overlap in a straight line) and survived longer as compared to animals treated with a single viral dose. Mice treated with a single IT or IV dose of MV-NIS still had significantly longer survival compared to the UV-inactivated controls ( $P < 0.05$ ).



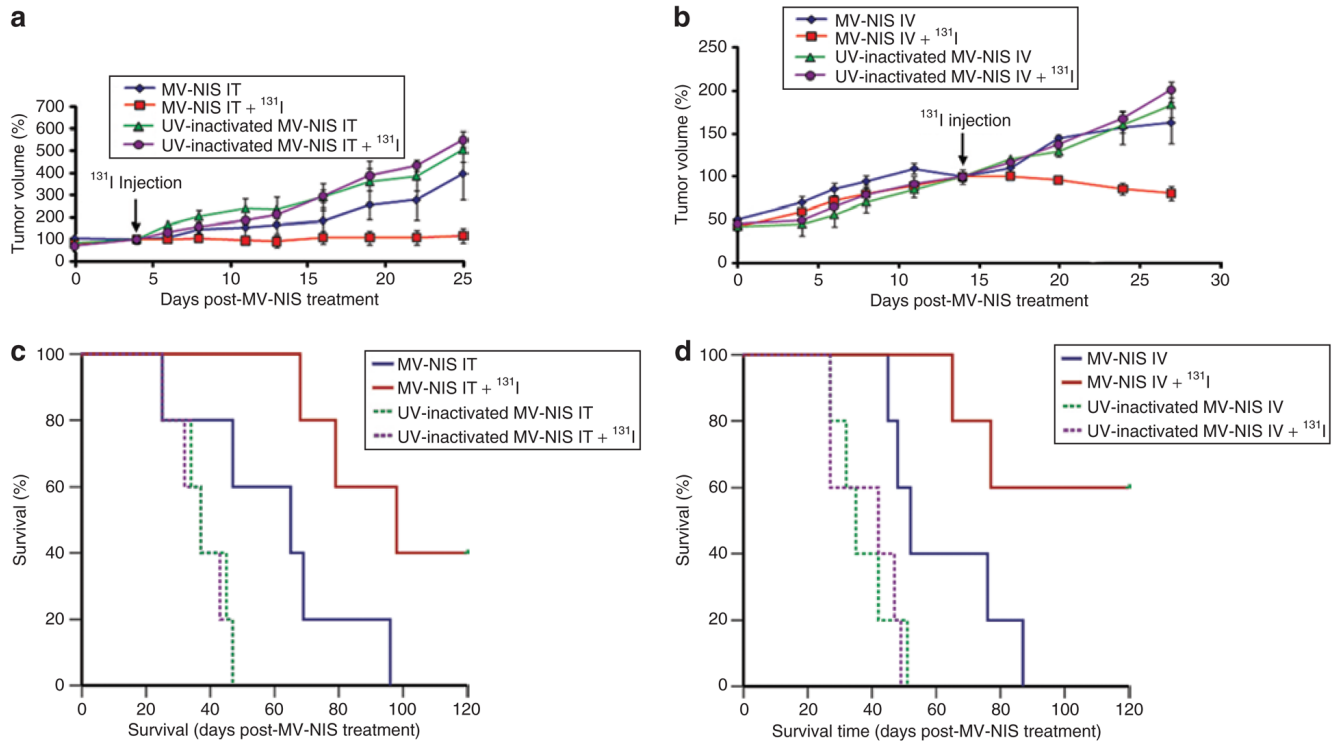


**Figure 6. Radiovirotherapy of prostate cancer tumors**

Mice ( $n = 5$  per group) bearing subcutaneous LNCaP xenografts received a single intratumoral (IT) or intravenous (IV) dose of  $1.5 \times 10^6$  TCID<sub>50</sub> measles virus–sodium iodide symporter (MV-NIS) or UV-inactivated MV-NIS with or without subsequent <sup>131</sup>I administration (1 mCi/mouse injected intraperitoneally 4 days after virus administration). There was significant suppression ( $P < 0.05$ ) of tumor growth in the combined IT radiovirotherapy group (a) at day 25 and in the combined IV radiovirotherapy group (b) at day 27 when the plots were censored because of deaths occurring in the control and single-agent treatment groups. Tumor volumes are expressed as the percentage relative to the values on the day of <sup>131</sup>I injection in each group and plotted against days after MV-NIS treatment. Points indicate mean; bars, SEM. (c) Mice in the IT radiovirotherapy group had significantly longer survival compared to the single-agent MV-NIS group ( $P < 0.05$ ). (d) Similarly, combined IV radiovirotherapy significantly increased survival compared to single-agent MV-NIS ( $P < 0.05$ ).